WCCM V
Fifth World Congress on
Computational Mechanics
July 7–12, 2002, Vienna, Austria
Eds.: H.A. Mang, F.G. Rammerstorfer,
J. Eberhardsteiner

The restricted influence of kinematic hardening on shakedown loads

M. Staat*

FH–Aachen Div. Jülich, Ginsterweg 1, D-52428 Jülich, Germany
e-mail: m.staat@fh-aachen.de

M. Heitzer

Central Institute for Applied Mathematics (ZAM)
Forschungszentrum Jülich GmbH, D-52425 Jülich, Germany
e–mail: m.heitzer@fz-juelich.de

Key words: shakedown, material shakedown, linear kinematic hardening, nonlinear kinematic hardening, ratchetting

Abstract
Structural design analyses are conducted with the aim of verifying the exclusion of ratcheting. To this end it is important to make a clear distinction between the shakedown range and the ratchetting range. In cyclic plasticity more sophisticated hardening models have been suggested in order to model the strain evolution observed in ratchetting experiments. The hardening models used in shakedown analysis are comparatively simple. It is shown that shakedown analysis can make quite stable predictions of admissible load ranges despite the simplicity of the underlying hardening models. A linear and a nonlinear kinematic hardening model of two-surface plasticity are compared in material shakedown analysis. Both give identical or similar shakedown ranges. Structural shakedown analyses show that the loading may have a more pronounced effect than the hardening model.

1 Introduction

Structural shakedown analysis is designed to exclude structural ratchetting which is produced by inhomogeneous stress fields [7]. Homogeneous fields are controlled by the behaviour of a representative material point. The analysis of uniaxial and biaxial stress cycles shows that the kinematic hardening is the primary reason for material ratchetting. Therefore, it is essential to develop and verify hardening rules which perform well under various cyclic loadings.

Classical shakedown analysis is based on the Melan-Prager linear kinematic hardening law [10], [11] which is known to be inadequate to simulate biaxial material ratchetting. The most well-known nonlinear kinematic hardening model has been proposed by Armstrong & Frederick [1]. Conceptually it is considered a leap in representing cyclic plasticity response of materials but not robust enough to predict the ratchetting response of materials [2]. Later, cyclic plasticity models have been suggested, which needed uniaxial and multiaxial cyclic tests for material characterization. Then the best could predict the amount of ratchetting in experiments which are close to the tests used for parameter identification. But all known models fail on one or more material ratchetting experiments. The large class of so-called coupled models fail conceptually to represent biaxial ratchetting if the material parameters are matched to the uniaxial tests and vice versa, because the uniaxial hardening modulus cannot be chosen independently of the kinematic hardening [2]. More flexibility is offered by the Dafalias & Popov two-surface model. Common to all modern models is that they need many parameters, which have to be determined in several cyclic tests. Parameter determination is vague for some models. Other models need uniaxial or biaxial ratcheting tests or try to formulate the anisotropic deformation of the yield surface [2]. Such effort is prohibitive for most industrial applications.

Shakedown analysis of cyclic structural plasticity needs only few characteristic material parameter and only the bounds of the load history. But it is regularly suggested that the simple constitutive models in shakedown analysis cannot represent the complexity which is observed in cyclic plasticity. In a first step numerical shakedown analysis has been extended to a simple two-surface plasticity model with fixed bounding surface by [5], [17] [18]. Shakedown theorems for the Armstrong & Frederick model have been proposed in [13], [3]. Fig. 1 suggests that these modern shakedown theorems are still not adequate for a ratchetting check. The paper considers examples for material and structural shakedown to demonstrate the amount of uncertainty that has to be expected with existing shakedown theorems.

2 Kinematic hardening models

2.1 The Melan-Prager linear kinematic hardening model

The original Melan-Prager model is characterized by unbounded translation of the loading surface in the multiaxial stress space [10], [11]:

$$F[\boldsymbol{\sigma} - \boldsymbol{\pi}] \leq \sigma_y^2, \tag{1}$$

$$\dot{\boldsymbol{\pi}} = \frac{2}{3} C \dot{\boldsymbol{\varepsilon}}^p = \frac{2}{3} \dot{\lambda} C \frac{\partial \sqrt{F}}{\partial \boldsymbol{\sigma}}, \tag{2}$$

with the associated plastic flow

$$\dot{\boldsymbol{\varepsilon}}^p = \dot{\lambda} \frac{\partial \sqrt{F}}{\partial \boldsymbol{\sigma}}. \tag{3}$$

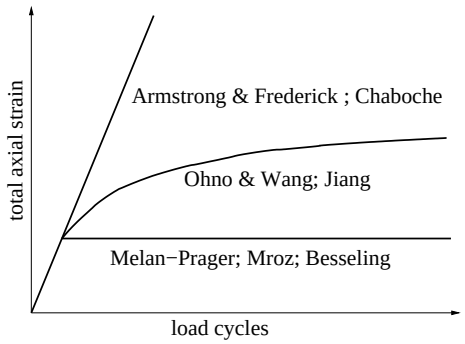

Figure 1: Capability of hardening models to describe strain evolution in uniaxial ratchetting (qualitatively after [14], [15]); experiments are typically close to the Ohno & Wang, Jiang curve.

The interior of the loading surface $\left\{\boldsymbol{\sigma} \mid F[\boldsymbol{\sigma}-\boldsymbol{\pi}] < \sigma_y^2\right\}$ is the elastic domain which is described by the function F and the yield stress σ_y. The von Mises function $F[\boldsymbol{\sigma}] = 3/2\ \boldsymbol{\sigma}^D : \boldsymbol{\sigma}^D$ with the deviatoric stress $\boldsymbol{\sigma}^D$ is used. The movement of the yield surface $F[\boldsymbol{\sigma}] \leq\ \sigma_y^2$ by the backstress evolution $\dot{\boldsymbol{\pi}}$ and the plastic flow $\dot{\boldsymbol{\varepsilon}}^p$ are both parallel and normal to the yield surface in this model. Backstress $\boldsymbol{\pi}$ and plastic strain $\boldsymbol{\varepsilon}^p$ are both deviators if F is the von Mises function. The uniaxial hardening modulus is $H = C$. The linear kinematic hardening always stabilizes to shakedown of homogeneous stress fields after some initial overprediction of ratchetting [2] (see Fig. 1).

2.2 The bounded linear kinematic hardening model

For realistic materials the stress $\boldsymbol{\sigma}$ is bounded by the ultimate stress σ_u. This is achieved by restricting the translation of the yield surface such that it always stays inside a bounding surface. In a simple two-surface model the bounding surface is described by the same von Mises function and it does not translate or deform in stress space. This is characterized by the additional constraint

$$F[\boldsymbol{\sigma}] \leq \sigma_u^2. \tag{4}$$

The elastic domain remains always in the limit surface and any stress $\boldsymbol{\sigma}$ in it may be reached if and only iff

$$F[\boldsymbol{\pi}] \leq (\sigma_u - \sigma_y)^2. \tag{5}$$

In a monotonic tension test σ_y and σ_u may be identified by $R_{p0.2}$ and R_m, respectively. But for cyclic experiments material parameters from a stable hysteresis curve may be more appropriate.

2.3 The Armstrong & Frederick nonlinear kinematic hardening model

The Armstrong & Frederick model introduces a recall term $-\zeta\boldsymbol{\pi}|\dot{\boldsymbol{\varepsilon}}^p|$ for the fading memory

$$\dot{\boldsymbol{\pi}} = \frac{2}{3}C\dot{\boldsymbol{\varepsilon}}^p - \zeta\boldsymbol{\pi}|\dot{\boldsymbol{\varepsilon}}^p|, \tag{6}$$

with the non-associated plastic flow

$$\dot{\boldsymbol{\varepsilon}}^p = \dot{\lambda}\frac{\partial f}{\partial \boldsymbol{\sigma}} \ \text{ and } \ |\dot{\boldsymbol{\varepsilon}}^p| := \sqrt{\frac{2}{3}\dot{\boldsymbol{\varepsilon}}^p : \dot{\boldsymbol{\varepsilon}}^p} \tag{7}$$

with

$$f = \sqrt{F[\boldsymbol{\sigma} - \boldsymbol{\pi}]} + \frac{3}{4}\frac{\boldsymbol{\pi} : \boldsymbol{\pi}}{\pi_u} \leq \sigma_u. \tag{8}$$

The uniaxial hardening modulus is $H = C - \zeta\pi\text{sign}(\sigma - \pi)$. Then $\pi_u = C/\zeta$ denotes the ultimate shift of the center of the initial yield surface $F[\boldsymbol{\sigma}] = \sigma_y^2$ in a uniaxial tension test, such that $\sigma_u = \sigma_y + \pi_u$ and $F[\boldsymbol{\pi}] \leq \pi_u^2$. This is again a two-surface model. The same bounding surface (4) is assumed asymptotically by the kinematic evolution rule (6) with $\dot{\boldsymbol{\pi}}$ no more proportional to the plastic flow $\dot{\boldsymbol{\varepsilon}}^p$.

Let $\boldsymbol{n}$ be the outward normal to the yield surface at the current stress point $\boldsymbol{\sigma}$. Let $\boldsymbol{\sigma}_L$ be the stress state on the bounding surface with the same outward normal $\boldsymbol{n}$. Then it holds

$$\boldsymbol{n} = \frac{\boldsymbol{\sigma}_L^D}{\sigma_u} = \frac{\boldsymbol{\sigma}_L^D - \boldsymbol{\pi}}{\sigma_y} \tag{9}$$

The model turns out to be a particular two-surface Mróz kinematic hardening model with a shift of the yield surface by

$$\dot{\boldsymbol{\pi}} = \zeta(\boldsymbol{\sigma}_L^D - \boldsymbol{\sigma}^D)|\dot{\boldsymbol{\varepsilon}}^p| \tag{10}$$

in deviatoric stress space. The shakedown theory has been extended to the Armstrong & Frederick hardening law in [13], [3].

3 Material shakedown analysis

Cyclic plasticity models are checked against the behaviour of homogeneous stress states, which can be represented by any material point. So called material ratchetting is caused by the material behaviour due to the nonproportional loading and may be analyzed by consideration of the movement and deformation of the yield surface. We suggest material shakedown analysis as a simplified method which only considers the stabilized state and avoids the detailed analysis of the whole deformation process.

Consider a constant tension with σ_N followed by a cyclic torsion with shear stress τ. Plastic flow $\dot{\boldsymbol{\varepsilon}}^p = (\dot{\varepsilon}^p, \frac{1}{\sqrt{3}}\dot{\gamma}^p)$ starts if the stress point $\boldsymbol{\sigma} = (\sigma_N, \sqrt{3}\tau)$ lies on the yield surface. The originally unbounded Melan-Prager model ($\sigma_u \to \infty$) is quite unrealistic. For a cyclic loading with nonzero mean value no finite shakedown load and no finite limit load is found. In contrast to this, the material always shakes down for fully reversed cycles with a load amplitude at yield stress once the backstress has achieved the constant stress (σ_N or τ_N). Damage is caused by LCF for larger cycles.

Obviously the bounding surface $F[\boldsymbol{\sigma}] \leq \sigma_u^2$ is the key to a realistic modeling of the shakedown behaviour. Ratchetting of the axial component $\dot{\varepsilon}^p$ stops if the yield surface touches the bounding surface in stress point σ_L. This elastic shakedown situation is constructed for the bounded Melan-Prager model and the Armstrong & Frederick model in Fig. 2(a) and Fig. 2(b). The stress points at shakedown are denoted σ_{mp} and σ_{af} for the bounded Melan-Prager and the Armstrong & Frederick model, respectively. The figures also show the backstresses π_{mp} and π_{af} for both models at shakedown.

1. For the tension-torsion shakedown experiment with constant tension σ_N and nonzero mean torsion Fig. 2(a) shows that both hardening models lead to the same material shakedown limit of the maximum shear stress $\tau_{max} < \tau_L$,

$$\tau_L = \frac{1}{\sqrt{3}}\sqrt{\sigma_u^2 - \sigma_N^2}. \tag{11}$$

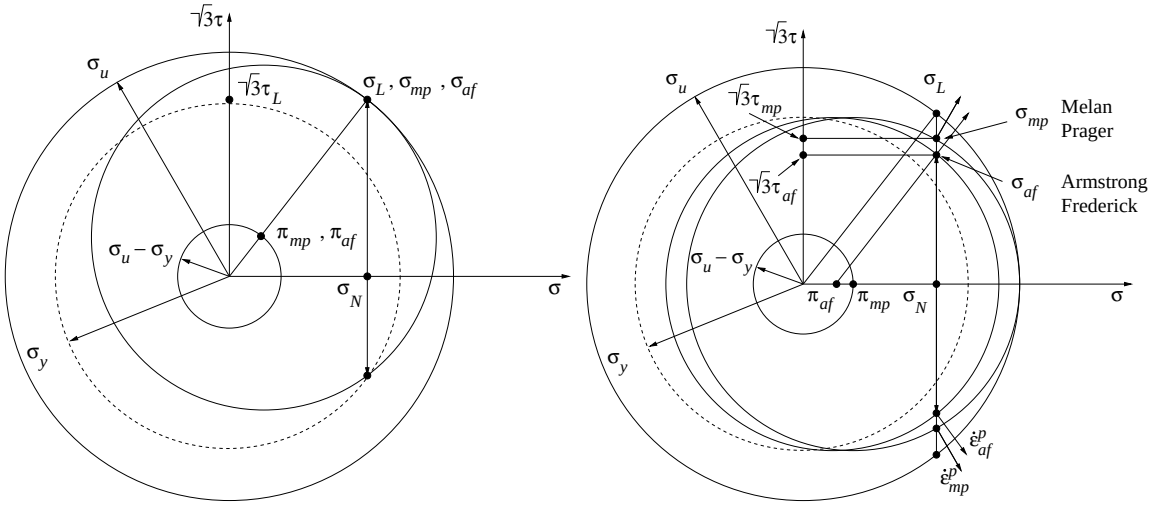

(a) Torsion with nonzero mean shear stress.

(b) Fully reversed torsion with zero mean shear stress.

Figure 2: Constant tension and cyclic torsion.

The solution is valid for any cyclic torsion with a minimum shear stress $\tau_{min} > \tau_L(\sigma_u - 2\sigma_y)/\sigma_u$. There is no difference between structural shakedown and material shakedown for the homogeneous stress state in pure tension. As observed for structural shakedown also the material shakedown stress coincides with the stress at instantaneous plastic collapse at limit load, because the points σ_{mp} and σ_{af} coincide with σ_L on the bounding surface.

2. A difference between the linear and the nonlinear kinematic hardening model may be observed in an experiment with fully reversed torsion cycles with zero mean shear stress ($\tau_{min} = -\tau_{max}$). For constant tension σ_N the material shakedown condition for the bounded Melan-Prager model with $\sigma_u < 2\sigma_y$ in Fig. 2(b) is

$$\tau_{mp} = \begin{cases} \frac{1}{\sqrt{3}}\sigma_y & \text{for} \quad 0 \le \sigma_N \le \sigma_u - \sigma_y, \\ \frac{1}{\sqrt{3}}\sqrt{\sigma_y^2 - (\sigma_N + \sigma_y - \sigma_u)^2} & \text{for} \quad \sigma_u - \sigma_y < \sigma_N \le \sigma_u. \end{cases} \tag{12}$$

The construction of Fig. 2(b) shows that the material shakes down like an unbounded hardening material for $\sigma_u \ge 2\sigma_y$.

For the Armstrong & Frederick model a result of Lemaître and Chaboche (1995) is obtained for constant tension σ_N and fully reversed torsion ($\tau_m = 0$) in Fig. 2(b)

$$\tau_{af} = \frac{1}{\sqrt{3}}\frac{\sigma_y}{\sigma_u}\sqrt{\sigma_u^2 - \sigma_N^2} = \frac{\sigma_y}{\sigma_u}\tau_L. \tag{13}$$

It is derived from structural shakedown analysis in [3]. The material shakedown load is below limit load for both models except for pure tension. For pure shear no material shakedown may be achieved with amplitudes beyond $1/\sqrt{3}\sigma_y$ for both models.

On a material level elasticity is any history in the interior of the initial yield surface. The boundary of the purely elastic range $F[\boldsymbol{\sigma}] < \sigma_y^2$ can be read as the equation $\sqrt{3}\tau + \sigma = \sigma_y$ of the dotted circle in Fig.

2(a) and Fig. 2(b). The only difference between elasticity and elastic material shakedown is that the latter is any history in the interior of the shifted yield surface (loading surface) $F[\boldsymbol{\sigma} - \boldsymbol{\pi}] < \sigma_y^2$. Therefore, a distinction can only be made if the nature of the surface is known. For this the backstress needs to be known with kinematic hardening models. But the backstress is not an observable quantity. Therefore, no difference between elastic shakedown and elasticity can be made in a continuum theory if the existence of a yield surface is accepted.

Material limit load is assumed if $F[\boldsymbol{\sigma}] = \sigma_u^2$. It is the solution of the equation $\sqrt{3}\tau + \sigma = \sigma_u$ of the outer circle in Fig. 2(a) and Fig. 2(b). Both hardening models predict material shakedown for cyclic stress with nonzero mean value up to material limit load. Eq. (11) makes no distinction between unlimited ratchetting and plastic collapse for this biaxial loading. In contrast to it another behaviour shows up with fully reversed stress cycles. For both models separated stress regimes exist with distinct material behaviour: elastic, shakedown, ratchetting, and collapse. Similarly to structural shakedown analysis no details of the load history are needed and material characterization is simplified to the knowledge of σ_y and σ_u. In tension torsion loading there is no or only little difference in the shakedown behaviour between a bounded linear and a nonlinear kinematic hardening material model. But the shakedown limits change noticeably with the load domains. This is also typically observed in structural shakedown analyses (see e.g. the interaction diagram of a pipe junction in [16].

4 Structural shakedown formulation

4.1 Shakedown theorem for bounded linear kinematic hardening material

Static shakedown theorems are formulated in terms of stress and define safe structural states giving an optimization problem for safe load regimes. The maximum safe load regime is the shakedown load regime avoiding ratchetting and low cycle fatigue. Any admissible solution of the static theorem is a true lower bound to the safe load regime. A body shakes down elastically for the given history of loading $\mathbf{P}(t)$ varying in load regime $\mathcal{L}$ if the plastic strains $\boldsymbol{\varepsilon}^p(t)$ become stationary, i.e.

$$\lim_{t\to\infty} \dot{\boldsymbol{\varepsilon}}^p(\mathbf{x},t) = \mathbf{0}, \quad \forall\, \mathbf{x} \in V. \tag{14}$$

and the total plastic energy dissipation W_p in the structure for the whole load history is bounded,

$$W_p = \int_0^\infty \int_V \boldsymbol{\sigma}(\mathbf{x},t) : \dot{\boldsymbol{\varepsilon}}^p(\mathbf{x},t) dx dt < \infty. \tag{15}$$

Therefore, a body shakes down if independent of the loading history the body approaches asymptotically an elastic limit state. The extended static theorem of shakedown for a bounded kinematic hardening material can be formulated as follows [5], [17]:

> If there exist a time–independent backstress field $\boldsymbol{\pi}(\mathbf{x})$ satisfying
>
> $$F[\boldsymbol{\pi}(\mathbf{x})] \leq (\sigma_u(\mathbf{x}) - \sigma_y(\mathbf{x}))^2, \tag{16}$$
>
> a factor $\alpha > 1$ and a time–independent residual stress field $\boldsymbol{\rho}(\mathbf{x})$ such that
>
> $$F[\alpha \boldsymbol{\sigma}^E(\mathbf{x},t) + \boldsymbol{\rho}(\mathbf{x}) - \boldsymbol{\pi}(\mathbf{x})] \leq \sigma_y^2(\mathbf{x})) \tag{17}$$
>
> holds for all possible loads $\mathbf{P}(t) \in \mathcal{L}$ and for all material points $\mathbf{x}$, then the structure will shake down elastically under the given convex load domain $\mathcal{L}$.

The time history of a load $\boldsymbol{P}(t) = (\boldsymbol{q}(t), \boldsymbol{p}(t))$ is often not well-known. It can however usually be stated that the loads (e.g. mechanical and thermal loads) vary only within a certain convex load domain $\mathcal{L}$. Typically, $\mathcal{L}$ is given by amplitudes or admissible bounds. If N_L is the number of corners $\boldsymbol{P}_1, \ldots, \boldsymbol{P}_{N_L}$ of $\mathcal{L}$, then all loads $\boldsymbol{P}(t) \in \mathcal{L}$ can be represented as convex combination with $0 \leq \lambda_j(t)$

$$\boldsymbol{P}(t) = \lambda_1(t)\boldsymbol{P}_1 + \ldots + \lambda_{N_L}(t)\boldsymbol{P}_{N_L}, \ \sum_{j=1}^{N_L} = \lambda_j(t) = 1.$$

The load-carrying capacity is exhausted by enlargement of $\mathcal{L}$ with the factor $\alpha > 1$ causing LCF, ratchetting or collapse. The shakedown theory analyzes only the shakedown state. It is sufficient to satisfy the shakedown conditions only in the N_L corners $\boldsymbol{P}_1, \ldots, \boldsymbol{P}_{N_L}$ of $\mathcal{L}$ if $\mathcal{L}$ is a convex set, because the shakedown theorems lead to convex optimization problems.

The greatest value α_{sd} for which the theorem holds is called shakedown-factor. This lower bound approach leads to the convex optimization problem

$$\begin{aligned}
\max \quad & \alpha && && (18)\\
\text{s.t.} \quad & F[\alpha\boldsymbol{\sigma}_j^E + \boldsymbol{\rho} - \boldsymbol{\pi}] \leq \sigma_y^2 && \text{in} \quad V, \ j = 1, \ldots, N_L && (19)\\
& F[\boldsymbol{\pi}] \leq (\sigma_u - \sigma_y)^2 && \text{in} \quad V && (20)\\
& \operatorname{div} \boldsymbol{\rho} = \mathbf{0} && \text{in} \quad V && (21)\\
& \boldsymbol{\rho}\,\mathbf{n} = \mathbf{0} && \text{on} \quad \partial V_\sigma && (22)
\end{aligned}$$

with infinitely many constraints, which can be reduced to a finite problem by FEM discretization. By use of the Besseling overlay material model it can be shown that the theorem holds for any stress strain curve [17]. Shakedown theorems for the Armstrong & Frederick model have been suggested in [13], [3].

Shakedown analysis gives the largest range in which the loads may safely vary with arbitrary load history. If the load regime $\mathcal{L}$ shrinks to a single load point, limit analysis is obtained as a special case. For the perfectly plastic behaviour ($\sigma_u = \sigma_y$), the backstresses $\boldsymbol{\pi}$ are identical to zero due to inequality (20). Melan's original theorem ([10]) for unbounded kinematic hardening can be also deduced from the previous formulation if $\sigma_u \to \infty$. Then inequality (20) is not relevant anymore and the backstresses $\boldsymbol{\pi}$ are free variables.

4.2 Discretization and Optimization

The shakedown theorems formulated for the continuum can be discretized by the FEM or they can be deduced directly for a discretized structure. For the FEM the structure V is decomposed in NE finite elements with the NG Gaussian points. The constraints of the optimization problem are satisfied only in the Gaussian points.

The number of Gaussian points becomes huge for industrial structures and no effective solution algorithms for the nonlinear optimization problem are available. A method for handling such large–scale optimization problems called basis reduction technique, was used in [17], [4], [5]. This basis reduction technique generalizes the line search technique, well–known in optimization theory. Instead of searching the whole feasible region for the optimum a search direction (a subspace with a small dimension) is chosen and one searches for the best value in this direction. The basis of the subspaces are generated by the general purpose Finite Element Code PERMAS [6], [8]. The basis reduction and the subspace iteration

technique described [4], [17] for perfectly plastic material cannot be directly applied to the shakedown problem for bounded kinematic hardening model. Therefore, in [5] a method for arbitrary 3–dimensional finite elements has been proposed for a bounded kinematic hardening material law.

4.3 Shakedown analysis of a tension torsion experiment

The shakedown domain for the FEM-model with HEXE20 [8] elements (Fig. 3(a)) was computed by the basis-reduction method for constant tension and cyclic torsion with zero mean stress. The geometry of the specimen is taken from [12] with $R_a = 12.7$cm and $R_i = 11.17$cm. The interaction diagram (Fig. 3(b)) for kinematic hardening material with $\sigma_u = 1.3\sigma_y$ is normalized by the pure shakedown tension N_{z0} and by the pure shakedown moment M_{z0} for perfectly plastic material with yield stress σ_y. The convex load domain $\mathcal{L}$ is generated by the constant load N and the load vertices M and $-M$, such that the elastic stresses $\boldsymbol{\sigma}^E$ for every load in $\mathcal{L}$ are given by $\boldsymbol{\sigma}^E = \boldsymbol{\sigma}^E_N + \mu(\boldsymbol{\sigma}^E_M) + (1-\mu)(-\boldsymbol{\sigma}^E_M)$. The

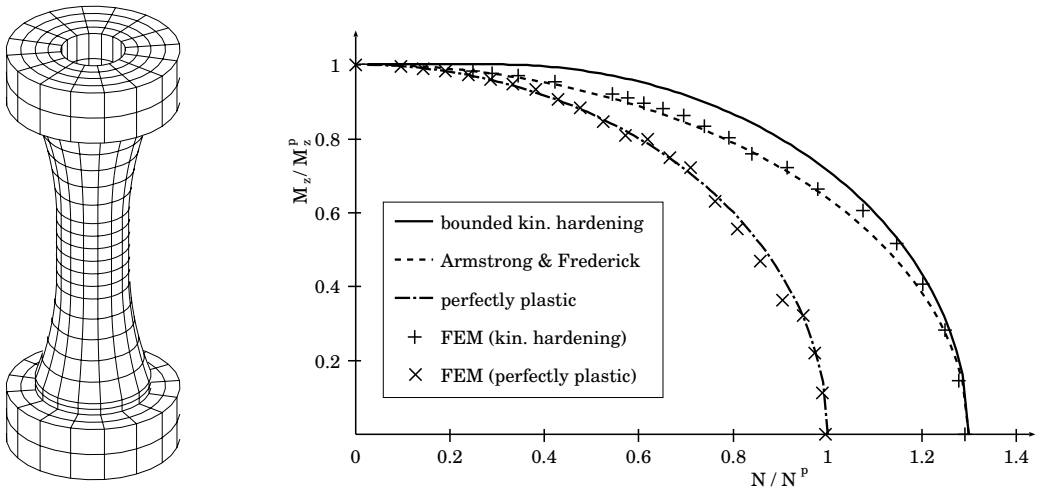

(a) FEM mesh

(b) Material shakedown interaction diagram

Figure 3: FEM mesh and material shakedown interaction diagram for fully reversed tension loading, normalized by the shakedown tension N^p and shakedown moment M_z^p for perfectly plastic material.

interaction diagram shows a significant safety benefit for the kinematic hardening law in comparison to the perfectly plastic shakedown domain. Other examples for this effect (including thermally loaded structures) are given in [5].

4.4 Shakedown analysis of a rotating disc

A turbine disc with uniform thickness rotates around its axis at an angular velocity ω. A radial temperature distribution $T(r) = \frac{r^2}{R^2}T^R$ with outer radius R is applied. Twenty axisymmetrical ring elements with quadrilateral cross section QUAX9 [8] are used for the discretization. Due to the symmetry of the problem only the upper half of the turbine is considered. The load factors corresponding to the elastic, the perfectly plastic and the bounded kinematic hardening behavior were computed for different ratios of ω and T^R. The load domain $\mathcal{L}$ has four load vertices $\mathbf{P}(1) = (\omega^2, 0),\ \mathbf{P}(2) = (0, T^R),\ \mathbf{P}(3) = (\omega^2, T^R),\ \mathbf{P}(4) = (0,0)$. The enlarged domain $\alpha\mathcal{L}$ is completely determined by the

load vertex $\left(\alpha\omega^2, \alpha T^R\right)$. The points $\left(\alpha\omega^2, \alpha T^R\right)$ where α is the corresponding computed load factor, are represented for different ratios of ω^2 and T^R. The obtained numerical results are shown in Fig. 4. Fig. 4 shows that the same finite shakedown load as for unbounded hardening is assumed for $\sigma_u \geq 2\sigma_y$.

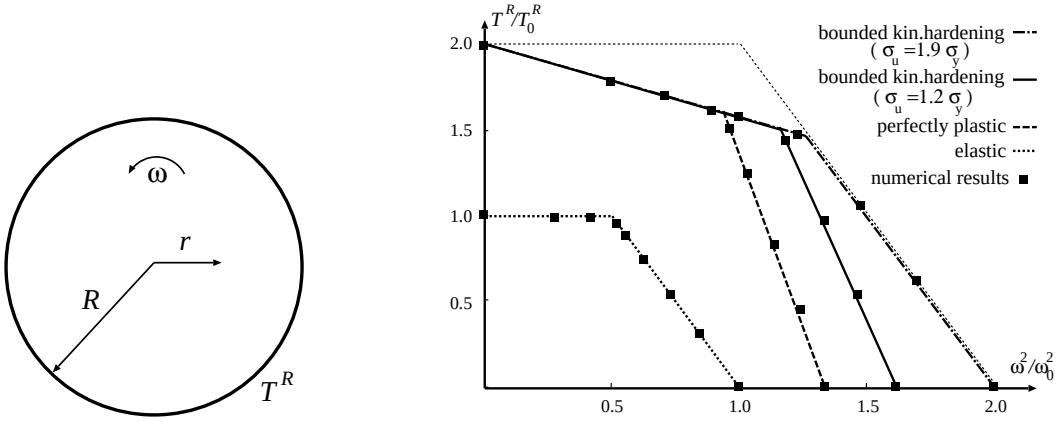

Figure 4: Structural shakedown diagram for a turbine disc

There is a range of ω where the LCF limit is independent on the hardening. The shakedown range is twice the elastic range for local failure under proportional loading.

5 Summary

Limit and shakedown analyses are simplified but exact methods of plasticity, which do not contain any restrictive prerequisites apart from sufficient ductility. The simplifications concern the details of material behaviour and of the load history. Shakedown analysis could be extended for a two-surface plasticity model of bounded linear kinematic hardening and to the Armstrong & Frederick nonlinear kinematic hardening model. For cyclic loading the linear and nonlinear kinematic hardening models exhibit quite distinct ratchetting behaviour but they predict the same or quite similar shakedown ranges.

In contrast to this, the shakedown limits change noticeably with the load domains. The shakedown range is the minimum of the collapse limit and twice the elastic range, for local macroscopic plastic failure under proportional loading. This result holds for perfectly plastic material as well as for unbounded kinematic hardening. Also the structural influence of a nonhomogeneous stress field may have a larger influence than the differences in the considered hardening models.

Acknowledgements

The research has been partly funded by the European Commission as part of the Brite–EuRam III project LISA: FEM–Based Limit and Shakedown Analysis for Design and Integrity Assessment in European Industry (Project N°: BE 97–4547, Contract N°: BRPR–CT97–0595).

References

[1] P.J. Armstrong, C.O. Frederick, *A Mathematical Representation of the Multiaxial Bauschinger Effect*, Central Electricity Generating Board Report No. RD/BN/N 731 (1966).

[2] S. Bari *Constitutive Modeling for Cyclic Plasticity and Ratcheting*, Ph.D. Thesis, North Carolina State University, Raleigh (2001).

[3] G. De Saxce, J.-B. Tritsch, M. Hjiaj, M., 2000. *Shakedown of elastic-plastic structures with nonlinear kinematical hardening by the bipotential approach*, in D. Weichert, G. Maier eds., *Inelastic Analysis of Structures under Variable Loads*, Kluwer, Dordrecht, (2000), pp. 167–182.

[4] M. Heitzer, *Traglast- und Einspielanalyse zur Bewertung der Sicherheit passiver Komponenten*, Berichte des Forschungszentrums Jülich, Jül–3704, Jülich, Germany (1999).

[5] M. Heitzer, G. Pop, M. Staat, M., *Basis reduction for the shakedown problem for bounded kinematic hardening material*, J. Global Optimization, 17, (2000), 185-200.

[6] M. Heitzer, M. Staat, M., 1999, *FEM–computation of load carrying capacity of highly loaded passive components by direct methods*, Nuclear Engineering and Design, 193, (1999), 349–358.

[7] H. Hübel, 1996. *Basic Conditions for Material and Structural Ratcheting*, Nuclear Engineering and Design, 162, (1996), 55–65.

[8] Intes, *PERMAS User's Reference Manuals*, Intes Publications No. 202, 207, 208, 302, UM 404, UM 405, Stuttgart, Germany (1988).

[9] J. Lemaitre, J.-L. Chaboche,*Mechanics of Solid Materials*, University Press, Cambridge (1990).

[10] E. Melan, E., *Zur Plastizität des räumlichen Kontinuums*, Ingenieur–Archiv, 8, (1938), 116–126.

[11] W. Prager, W., 1956. *A New Method of Analyzing Stresses and Strains in Work Hardening Plastic Solids*, J. Applied Mechanics, 23, (1956), 493–496.

[12] L. Portier, S. Calloch, D. Marquis, P. Geyer, *Ratchetting under tension-torsion loadings: experiments and modelling*. Int. J. Plasticity 16, (2000), 303–335.

[13] S. Pycko, G. Maier, *Shakedown theorems for some classes of nonassociated hardening elastic-plastic material models*, Int. J. Plasticity, 11, (1995), 367–395.

[14] S. Postberg, *Beitrag zum Ratchetting-Verhalten von Komponenten der Druckbehälter- und Kraftwerkstechnik*, Shaker Verlag, Aachen (2000).

[15] M. Sester, R. Mohrmann, R. B¨oschen, *Ratcheting of an austenitic steel under multiaxial and thermomechanical loading: experiments and Modelling*, in K.-T. Rie, P.D. Portella, eds., *Low Cycle Fatigue and Elasto-Plastic Behaviour of Materials*, Elsevier, Amsterdam, (1998), pp. 647–652.

[16] M. Staat, M. Heitzer, *LISA a European Project for FEM-based Limit and Shakedown Analysis*, Nuclear Engineering and Design, 206, (2001), 151–166.

[17] E. Stein, G. Zhang, R. Mahnken, *Shakedown analysis for perfectly plastic and kinematic hardening materials*, in E. Stein, ed., *Progress in computational analysis of inelastic structures*, Springer, Wien, (1993), pp. 175–244.

[18] D. Weichert, J. Gross-Weege, *The numerical assessment of elastic-plastic sheets under variable mechanical and thermal loads using a simplified two-surface yield condition*, Int. J. Mec. Sci., 30, (1988), 757-767.